Evaluation of Human Control in Teleoperation of Underwater Vehicles - Compative Study in Time and Frequency Domains

Mario A. Jordán [1,2], Jorge L. Bustamante[1,2] and Carlos Berger[1,2]

[1] Argentinean Institute of Oceanography (IADO-CONICET).
Florida 8000, Complejo CCT,
Edificio E1, B8000FWB, 8000 Bahía Blanca, ARGENTINA.

[2] Dto. Ingeniería Eléctrica y de Computadoras- Univ. Nac. del Sur
(DIEC-UNS).

Abstract. In this paper a study of teleoperation of remotely operated vehicles is carried out employing two sources of video, the inboard image and external camera. Additionally, a modeling of the human behavior during path tracking is performed. For this goal a structure of a nested control loop is supposed. The inner loop involves a high-performance digital controller, while the outer loop is composed by the human teleoperation. For modeling the human control actions a PID-like controller is proposed. The identification of the parameters of the PID is carried out in both domains, time and frequency. Features of these studies are based on experiments designed by simulations and on-line interaction of the teleoperator by means of a joystick.

Key words: Teleoperation - Remotely operated vehicles - Human control - Nested control loops - PID Control

1   Introduction

Commonly, in the teleoperation of ROVs (Remotely Operated Vehicles), there are many automation tasks on which the operator has to pay attention simultaneously according to the complexity of the mission. For instance, in the guidance of a ROV along marks or paths on the sea bottom adjusting simultaneously a specified altitude, or the tracking of a mobile target avoiding obstacles, or the regulation about a fixed point with parallel manipulation of a robotic arm, among other ones. In addition to the inboard camera the operator can have eventually the assistance of an external camera to perform the tasks as in the case of offshore applications .

From a control point of view, the vehicle teleoperation can be framed into a control structure with nested loops. These are an internal loop containing navigation autopilots for the ROV dynamics, and an external control loop of the human control for vision-based guidance. The key idea in the analysis of human control performance is to conceive the inner control loop as a wide-bandwidth

system in comparison with the outer closed loop which is dominant in dynamics an track smooth path references given as commands by the operator.

Usually, autopilots are designed for some vehicle motion modes such as pitch, roll, attitude and depth, and in some sense they contribute to unload the attention of the teleoperator paid in different tasks at the same time during the guidance, particularly by strong perturbations. In the case of path tracking the attention of the teleoperator would be concentrated in the course and cruise velocity above all while altitude or depth is regulated by the inner control loop. For this loop, many theoretical computer-based control algorithms were claimed to potentially provide a high performance in path tracking, indeed with adaptive, robust and intelligent features [1]-[3]. They are able to reject efficiently both perturbations of cable tugs and current disturbances.

The evaluation of the stability and performance of the nested control loop is a complex issue, mainly due to it depends on human skill, stage of learning in the teleoperation and the fatigue related with the time that the operator is in a particular task. Basically this dynamics is nonlinear, knowledge-dependent and time-varying.

A model of this control system would be certainly useful in numerical simulations for tasks scheduling and training in oceanographic missions and offshore applications. In these case, at least, a model of a skillful and refreshed teleoperator in a completed phase of his learning is desired.

Usually, contributions in human control depart from a linear modeling of all components. In [4] the Human balance response was analyzed by means of a PID controller, the PID parameters was adjusted in frequency fitting the experimental bode diagram with the bode obtained using a PID controller. In [5], a similar problem was analysed, considering the PID identification by measuring the Human behavior in time and using least square to adjust the PID parameters. In [6]-[7] the focus was the time delay of the human teleoperation and its effects on the control loop.

In this paper it is focused the modeling of a skillful teleoperator with behavior in a stationary stage interacting with a computer-model simulated ROV dynamics by means of a joystick and virtual motion images. An attempt to obtain PID parameters that characterizes his behavior is carried out, above all, during path tracking. The identification will be basically supported on both, time and frequency domain. Different sources of image motion are considered separately, namely bow camera (egomotion) and external camera.

2 Control-assisted teleoperation approach

A model of the teleoperation dynamics of a ROV guided by a skillful operator can be considered as being composed of visual sensors, calculation capability for decision-making and finally actuators. This is arranged in a two-nested-loops system as illustrated in Fig. 1.

Accordingly, let us denote first the main motion modes (states) for an underwater vehicle by the geometric position vector $\boldsymbol{\eta} = [x, y, z, \varphi, \theta, \psi]^T$ and the kinematics vector $\mathbf{v} = [u, v, w, r, p, q]^T$ (according to the notation in [8]). Moreover $\boldsymbol{\eta}$ is referred to an earth fixed coordinate systems, while $\mathbf{v}$ is defined with

respect to a body-fixed system oriented according to the vehicle main axes. From now on, we consider a motion in 6 DOFs and perturbations in all modes. In addition, $\overset{\smile}{\boldsymbol{\eta}}$ and $\overset{\smile}{\mathbf{v}}$ are path errors. The suffix "hr" denotes path references existing in the intention of the teleoperator for establishing desired position and cruise velocity; the suffix "h" is reserved for the states that are judged by the operator at any moment from motion image sequences screened on a monitor. Finally the suffix "r" means references for the inner control loop.
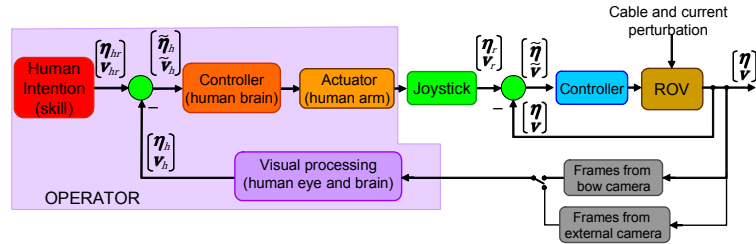

Fig. 1 - Nested control loops for teleoperation of a ROV

From the image processing the operator estimates position and kinematics and forces the vehicle to targets which are in his intention. This generates positioning and kinematics errors which demand at the same time corrections through joystick manipulations. Innerly path references for the internal fixed control system are created.

There exists a pure delay in the outer loop mainly due to the video transmission and its consideration is important for preserving stability. The human reaction delay is consider for an experienced teleoperator negligible. Besides the teleoperator may additionally have the assistance of an external camera (offshore applications) to improve the guidance in limited spaces [9].

We distinguish between modes that are full controlled by autopilots from modes that are controlled by the teleoperator. In the first group, there are the heave modus, the roll and pitch angles, and their rates. Commonly all them are set constant accomplishing for a certain depth and vehicle orientation. Teleoperator controlled modes are usually the displacements tangential and transversal to the path and the course rate. In other applications of the work-class ROVs the regulation problem about a point is more important than the navigation. In this case the dynamic positioning of the vehicle involves usually the pitch angle and position coordinates.

2.1 Teleoperation model

As mentioned in the introduction one can depart in the paper from a high-performance inner control loop whose response is commonly much more rapid than the response of the human control loop. So appearing disturbances are rejected or attenuated very rapid by the automatic guidance system so that the flow of energy from the inner control loop into the teleoperated modes is relatively negligible and described by short transients like parasitics.

Taken this fact in mind, we find a perturbed linear system as an adequate approximation of the dynamics of the controlled ROV. In such a case a good

model for the human control is a PID control [1]-[2]. Moreover an expert teleoperator has the ability to predict the image sequence delay. The structure of the modeled teleoperation is shown in Fig. 2.
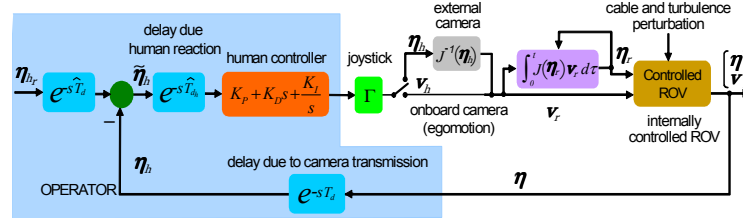

Fig. 2 - Model of teleoperated ROV with onboard and external cameras

Here, there are two pure delays, namely the one appeared in the video transmission T_d and the other originated in the human reaction T_{d_h}. Their estimation by part of the teleoperator after full training is indicated as $\hat{T}_d$ and $\hat{T}_{d_h}$. The matrices K_p, K_D and K_I accomplish for proportional, derivative and integral corrections. They are assumed diagonal and related to the teleoperated modes only. The joystick is modeled by a gain matrix affecting the rate vector in two different alternatives: 1) from egomotion (inboard camera) the vector $\mathbf{v}_h=\mathbf{v}_r$ is generated, or 2) from external camera the vector $\dot{\boldsymbol{\eta}}_h$ is created instead.

2.2 Control strategy

The teleoperator will apply his full skill to predict the position and rate of the vehicle compensating for the delays in video transmission and his proper delay for introducing the control action. So the teleoperation along a path succeed as illustrated in Fig. 3 for a linear stretch. In Fig 3, A), the real position mark $\triangledown$ is masked by the delay $T_d + T_{d_h}$, so the mark $\blacktriangledown$ is perceived instead. Moreover, the teleoperator is conscious of the intended position mark $\square$. So he attempts to delay this mark in the time $\hat{T}_d + \hat{T}_{d_h}$ at the place $\blacksquare$ and fixes the correction so that $\blacktriangledown$ coincides with $\blacksquare$. In the ideal situation B), the teleoperation reaches null error. This coincidence implies that the marks $\triangledown$ and $\square$ would be superposed too.
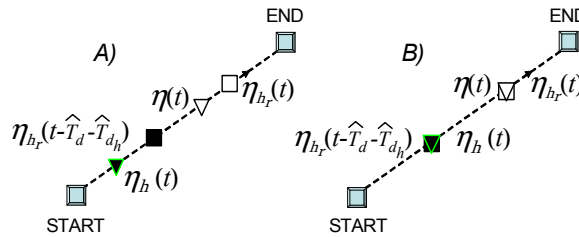

Fig. 3 - Teleoperation performance. A) Control with tracking errors. B) Ideal situation of null tracking errors

2.3 Internal fixed control

To design the internal control let us consider first the well-known ROV dynamics given by [8]

$$\dot{\mathbf{v}}=M^{-1}\left(-C(\mathbf{v})\mathbf{v}-D(|\mathbf{v}|)\mathbf{v}+\mathbf{g}(\boldsymbol{\eta})\right) + M^{-1}\left(\boldsymbol{\tau}_c + \boldsymbol{\tau}\right) \tag{1}$$

$$\dot{\boldsymbol{\eta}}=J(\boldsymbol{\eta})(\mathbf{v}+\mathbf{v}_c), \tag{2}$$

where $J(\boldsymbol{\eta})$ is the well-known rotation matrix, M is the inertia matrix, $C(\mathbf{v})$ is the centripetal and Coriolis matrix, $D(|\mathbf{v}|)$ is the damping matrix, $\mathbf{g}(\boldsymbol{\eta})$ is the net buoyancy force, $\boldsymbol{\tau}_c$ the cable tug, and $\boldsymbol{\tau}$ the generalized thrust. The actuators are operated with $\boldsymbol{\tau}$ to achieve the distribution on the the thrusters through

$$\mathbf{f}=B^T\left(BB^T\right)^{-1}\boldsymbol{\tau}, \tag{3}$$

where $\mathbf{f}$ is the thrust vector and B is a constant matrix with elements that depend of the ROV geometry.

We aim a controller that tracks references $\boldsymbol{\eta}_r(t)$ and $\mathbf{v}_r(t)$ (see Fig. 2) with asymptotic null errors for arbitrary bounded initial conditions $\boldsymbol{\eta}(0)$, $\mathbf{v}(0)$. Moreover we will require a flexible controller design in the sense that we are able to tune the transient performance of the inner control loop.

In [10] a digital speed-gradient control was developed with these features. It is designed for a digital model of the dynamics based on Adams-Bashforth approximations. For a first-order sampled-data model one attains

$$\mathbf{v}_{n+1} = \mathbf{v}_{t_n}+h\left(\mathbf{G}_{t_n}+M^{-1}\boldsymbol{\tau}_n\right)+\boldsymbol{\delta}_{v_n} \tag{4}$$

$$\boldsymbol{\eta}_{n+1} = \boldsymbol{\eta}_{t_n}+h\mathbf{H}_{t_n}+\boldsymbol{\delta}_{\eta_n}, \tag{5}$$

with

$$\mathbf{G}(\boldsymbol{\eta},\mathbf{v}) = M^{-1}\left(-C(\mathbf{v})\mathbf{v}-D(|\mathbf{v}|)\mathbf{v}+\mathbf{g}(\boldsymbol{\eta})\right) \tag{6}$$

$$\mathbf{H}(\boldsymbol{\eta},\mathbf{v},\mathbf{v}_c) = J(\boldsymbol{\eta})\mathbf{v} \tag{7}$$

$$\boldsymbol{\delta}_v = hM^{-1}\boldsymbol{\tau}_c+\boldsymbol{\varepsilon}_v \tag{8}$$

$$\boldsymbol{\delta}_\eta = hJ(\boldsymbol{\eta})\mathbf{v}_c+\boldsymbol{\varepsilon}_\eta, \tag{9}$$

where h is the sampling period, $\mathbf{v}_{n+1}$ and $\boldsymbol{\eta}_{n+1}$ are one-step-ahead predictions, $\mathbf{v}_{t_n}$, $\boldsymbol{\eta}_{t_n}$, $\mathbf{G}_{t_n}$ and $\mathbf{H}_{t_n}$ samples at present sampling time $t = t_n = nh$ with n a positive integer. Finally, $\boldsymbol{\varepsilon}_{v_n}$ and $\boldsymbol{\varepsilon}_{\eta_n}$ are bounded model errors of the digitalization.

For the first-order model the digital controller it is shown that the control action at time step n is

$$\boldsymbol{\tau}_n=M\left(-K_v\breve{\mathbf{v}}_{t_n}+\frac{1}{h}\left(-J_{t_n}^{-1}\dot{\boldsymbol{\eta}}_{r_{t_n}}+J_{t_{n+1}}^{-1}\dot{\boldsymbol{\eta}}_{r_{t_{n+1}}}-J_{t_{n+1}}^{-1}K_p\breve{\boldsymbol{\eta}}_{t_{n+1}}+J_{t_n}^{-1}K_p\breve{\boldsymbol{\eta}}_{t_n}\right)-\right. \tag{10}$$

$$\left.-\mathbf{G}_{t_n}-\frac{1}{2h^2}\mathbf{b}\pm\frac{1}{2h^2}\sqrt{\frac{\mathbf{b}^T\mathbf{b}-4h^2c}{6}}\mathbf{o}\right),$$

with $\breve{\mathbf{v}}_{t_n} = \mathbf{v}_{t_n}-J_{t_n}^{-1}\dot{\boldsymbol{\eta}}_{r_{t_n}}+J_{t_n}^{-1}K_p\breve{\boldsymbol{\eta}}_{t_n}$, $\breve{\boldsymbol{\eta}}_{t_n} = \boldsymbol{\eta}_{t_n}-\boldsymbol{\eta}_{r_{t_n}}$ and

$$\mathbf{b}^T = 2h\left((I - hK_v)\breve{\mathbf{v}}_{t_n}\right)^T \tag{11}$$

$$c = h^2\left(J_{t_n}\breve{\mathbf{v}}_{t_n}+\dot{\boldsymbol{\eta}}_{r_{t_n}}\right)^2 + h\left(J_{t_n}\breve{\mathbf{v}}_{t_n}+\dot{\boldsymbol{\eta}}_{r_{t_n}}\right)^T\left(\boldsymbol{\eta}_{r_{t_n}}-\boldsymbol{\eta}_{r_{t_{n+1}}}\right)+$$

$$+\left(\boldsymbol{\eta}_{r_{t_n}}-\boldsymbol{\eta}_{r_{t_{n+1}}}\right)^T\left(\boldsymbol{\eta}_{r_{t_n}}-\boldsymbol{\eta}_{r_{t_{n+1}}}\right) + 2\left(I - hK_p\right)\breve{\boldsymbol{\eta}}_{t_n}\left(h\left(J_{t_n}\breve{\mathbf{v}}_{t_n}+\dot{\boldsymbol{\eta}}_{r_{t_n}}\right)+\right.$$

$$\left.+\boldsymbol{\eta}_{r_{t_n}}-\boldsymbol{\eta}_{r_{t_{n+1}}}\right)$$

$$\mathbf{o} = [1,...,1]^T \tag{12}$$

and finally the tuning matrices $K_v = K_v^T \geq 0$ and $K_p = K_p^T \geq 0$ with restrictions

$$\frac{2}{h}I > K_p \geq 0 \tag{13}$$

$$\frac{2}{h}I > K_v \geq 0. \tag{14}$$

This control system is stable for (13)-(14) and its performance can be influenced by the choice of the tuning matrices K_p and K_v in this range. Guidelines for attaining a high performance are given in [10].

2.4   Model of the controlled ROV

If the ROV dynamics is perfectly modeled the perturbed controlled dynamics of the path and kinematic errors in analog form is ($cf.$[11])

$$\dot{\breve{\mathbf{v}}} = M^{-1}\Big(-K_v\breve{\mathbf{v}}-J^T(\boldsymbol{\eta})\breve{\boldsymbol{\eta}}+\boldsymbol{\tau}_c\Big) \tag{15}$$

$$\dot{\breve{\boldsymbol{\eta}}} = -K_p\breve{\boldsymbol{\eta}}+J(\boldsymbol{\eta})\breve{\mathbf{v}} + J(\boldsymbol{\eta})\mathbf{v}_c. \tag{16}$$

It is worth noticing that the design matrices K_v and K_p can influence this dynamics apart from the inertial perturbation $\boldsymbol{\tau}_c$ (cable tug) and kinematic perturbation $\mathbf{v}_c$ (sea current).

Clearly, this dynamics is nonlinear due to the terms containing $J(\boldsymbol{\eta})$. However, considering high-quality autopilots destined for the vehicle orientation, J can be considered as a constant matrix. Moreover, transients in the inner control loop can produce momentarily a non-null term $\frac{d}{dt}(J^{-1}(\boldsymbol{\eta})\mathbf{v}_c)$ in (15) which can be seen in our context as a bounded spurious disturbance.

Applying the digitalization procedure to (15)-(16) as in (4)-(5), the sampled-data model error of the perturbed controlled ROV dynamics is

$$\widetilde{\mathbf{v}}_{n+1} = \big(I - hM^{-1}K_v\big)\,\widetilde{\mathbf{v}}_{t_n}+\widetilde{\boldsymbol{\delta}}_{v_n} \tag{17}$$

$$\widetilde{\boldsymbol{\eta}}_{n+1} = \big(I - hK_p\big)\,\widetilde{\boldsymbol{\eta}}_{t_n}+\widetilde{\boldsymbol{\delta}}_{\eta_n}, \tag{18}$$

with the bounded disturbances $\widetilde{\boldsymbol{\delta}}_{v_n}$ and $\widetilde{\boldsymbol{\delta}}_{\eta_n}$ being given by

$$\widetilde{\boldsymbol{\delta}}_{v_n} =hM^{-1}\Big(-J_{t_n}^T\breve{\boldsymbol{\eta}}_{t_n}+\boldsymbol{\tau}_{c_n}\Big)+ \mathbf{F}_v(\boldsymbol{\varepsilon}_{\eta_n},\boldsymbol{\varepsilon}_{v_n}) \tag{19}$$

$$\widetilde{\boldsymbol{\delta}}_{\eta_n} =hJ_{t_n}\mathbf{v}_{t_n} + hJ_{t_n}\mathbf{v}_{c_n}+\mathbf{F}_\eta(\boldsymbol{\varepsilon}_{\eta_n},\boldsymbol{\varepsilon}_{v_n}), \tag{20}$$

with $\mathbf{F}_v$ being $\mathbf{F}_\eta$ are bounded error functions that appears in the digital control [12]. They depend on h and are of small magnitude. Moreover, it is noticing that samples of the perturbations $\mathbf{v}_c$ and $\boldsymbol{\tau}_c$ are present in $\widetilde{\boldsymbol{\delta}}_v$ and so they influence directly the path errors. Nevertheless they are strongly attenuated by the factor h and the inverse of the mass matrix whose induced norm is commonly very small in ROVs.

So the operator can rest on the inner control for a rapid and effective attenuation of the perturbations of current an cable tugs.

2.5 Model of the human control

Assuming the controlled ROV dynamics as described previously, we can consider the human control as one with superposed proportional, derivative and integral actions applied to the joystick. Additionally he attempts to predict the ROV response due to the camera and human-reaction delays.

One of the goals in this paper is to confirm the hypothesis of the PID-like predictive human control. To this end we attempt to identify the controller matrices K_P, K_D and K_I, T_d and T_{d_h} with simple experiments by means of simulated virtual image scenarios and interacting with the resulting image motion via joystick. Thereafter we will compare the simulated teleoperation with the interactive teleoperation for the same paths and control criterion (described in Fig. 3.)

3 Case study

Now, We considered the teleoperation along an intended planar flying path based on inboard and external image motions separately. In Fig 4 could be seen the visualization of image motion for both cases. The objective is to follow the marks that appear in the camera in a consecutive form, so that the teleoperator could conduct the ROV without confusion. The teleoperator was trained in the sought path trying that the guidance errors went to a minimum value in stationary sense.
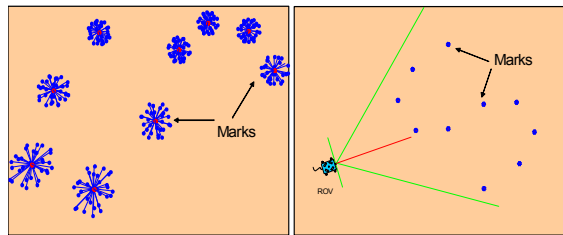

Fig. 4 - Visualization of image motion for teleoperation along an intended path with marks. Left: from onboard camera . Right: from external camera

To this end we simulate the dynamic of a full-actuated 6-DOFs ROV presented in [11]. The inner controller is programmed according to (10) with design matrices K_p and K_v given in Table 1. The outer human control is arranged by a joystick connected with the inner loop for on-line interaction. T_d and T_{d_h} can be easily estimated, the last one trying to measure the human response to sudden changes capture by the vision. Both considered delays are given in Table 1.

In the experiments, the vehicle is forced to navigate along the sequence of marks at a certain intended rate including advance velocity and rotation. The guidance is conduced along rectilinear segments until the vehicle reaches a mark. After that, the advance and rotation is performed at the same time until the following mark could be reached again using only the advance velocity in a linear segment.

The human control is performed for the teleoperated modes, namely u, v and r, while the rest of modes are innerly controlled by the controller algorithm

previously exposed. These modes involve the orientation of the vehicle and the altitude which are regulated constant.

In the following we present the identification of the PID parameters. This is achieved employing two different ways separately, namely, the identification in Time and in Frequency domain.

3.1 PID identification in Frequency Domain

For the identification in frequency domain it was considered a random path as the most practical way to excite a ROV dynamics in several frequencies at the same time. The irregularities of the path are sufficiently smooth and adequate to the response of a human control in its typically frequency band ($\omega < 0.3$ Hz.). The fast Fourier transform (FFT) was applied as measure of the teleoperation behavior in a context of path following. We construct a spectrum of the teleoperation together with a spectrum of a PID-control-like system that account for the human behavior. Here, an optimal PID controller was found by searching the best fit of spectra in a least-squares sense of the spectra error.

Particularly, for the x-mode with an external camera, the result of the frequency optimization is shown in Fig 5., left. Although it is noticed a great coincidence between both curves, the existing small errors at high frequencies ($\omega > 0.3$ Hz.) impact considerably in the errors in time domain. This property could be seen in Fig 5, right.
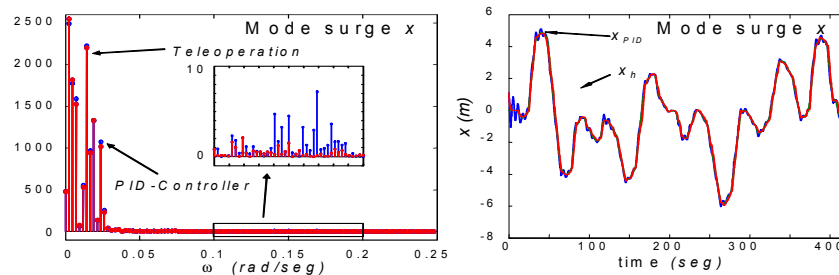

Fig 5 - Left: FFT of the evolution of the teleoperated x mode with external camera. Right: Time evolution of the teleoperated x mode (External camera, Human and PID-like control fit in frequency domain)

For that reason we had considered quite adequate (in second phase of experiments) to include a low pass filter after generating the position and cinematic references. So a suitable cut-off frequency was obtained for high frequency errors before estimating. With these results we find a much more tight fit of the spectra. It could find that this result is better than in the first case (see Fig 6, left). However, the filter in turn introduces an undesirable phase delay which had to be compensated. The result in the time domain is shown in Fig 6, right. First it was noticed that at lower frequencies, the phase delay is related to a time delay of the PID-like behavior curve with respect to the path reference. This difference in time could be counterbalanced by including a "time lead" in the references. Once this filter was included in the control structure we had preferred to continue the research the parameter identification in time instead in frequency domain.
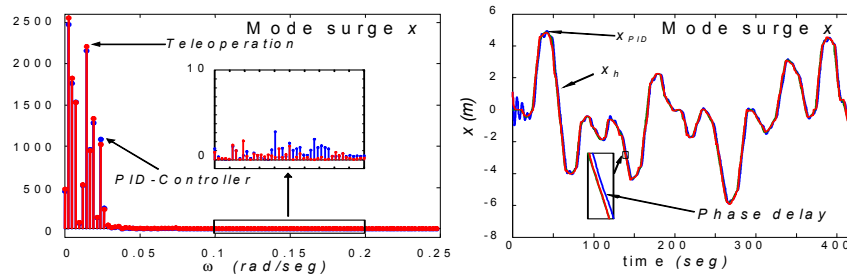
Fig 6 - Left: FFT of the evolution of the teleoperated x mode. Right: Time evolution of the teleoperated x mode (External Camera, Human and PID-control fit in frequency with low pass filter)

3.2 PID identification in Time Domain

For this goal we have taken into account a period 250 s and applied again the least-squares-based estimation method. As could be seen in (Fig 7, top), the fit is much better here than in the same case evaluated in frequency domain. In Fig 7 one see also the results for external camera in the other motion modes y (Fig 7, middle) and ψ (Fig 7, bottom). In the Fig. 8 a zoom on the curves in x, y, φ show stretches in time in which the PID-like behavior seems very similar to the human teleoperation.
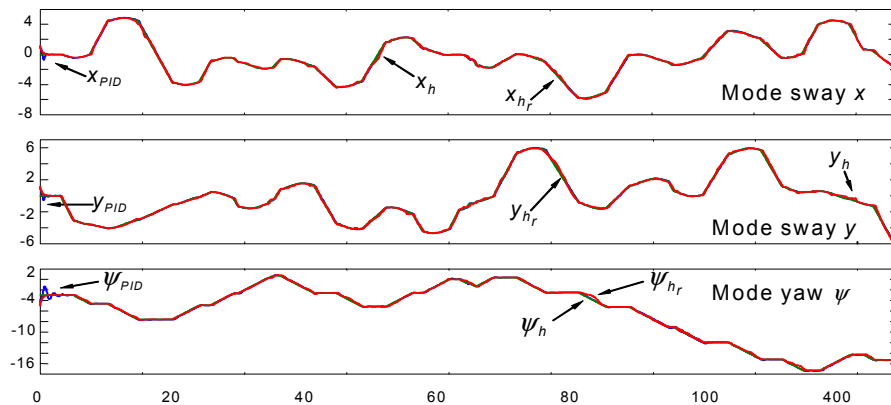

Fig. 7 - Time evolution of the teleoperated geometric states with external camera (Human and PID-like control fit in time domain)
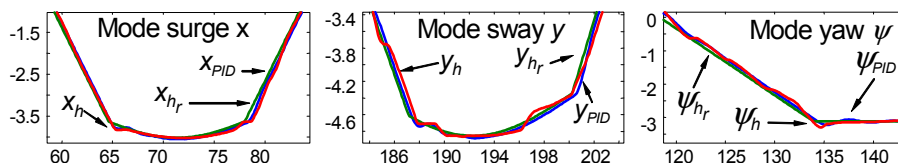

Fig. 8 - Comparison of time evolutions of geometric states with external camera (Human and PID-like control fit in time domain)

In Fig. 9 it is similar fits with inboard camera in the modes x, y and ψ are depicted. The comparative study shows quite similar as in the previous case in time domain.

In Table 1 the PID parameters obtained for the two studied camera cases are shown . In Table 2 we present the Means Square Error measured between the teleoperation and the PID controller in the Time interval considered to the Identification and in the Time interval corresponding to the rest of the simulated teleoperation. It could be seen that this error is not too different between the two Time Intervals.
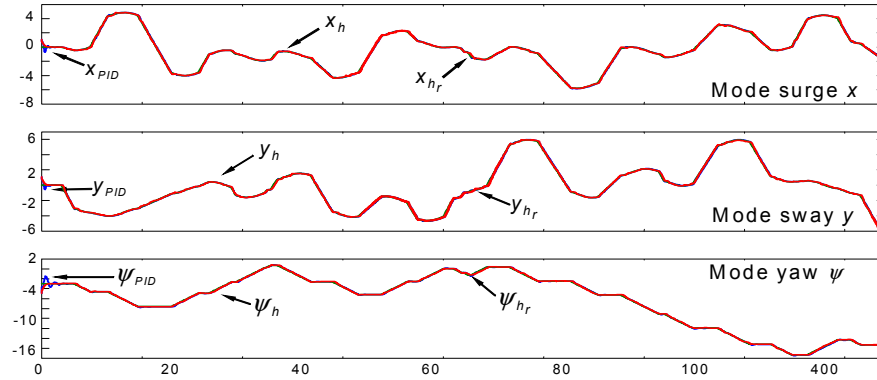

Fig. 9 - Time evolution of the teleoperated geometric states with inboard camera (Human and PID-like control fit in time domain)

Table 1 - Control parameters for teleoperation with nested control loops

$$K_p = \mathrm{diag}\,(1)$$
$$K_v = \mathrm{diag}\,(12)$$
$$h = 0.1(s)$$
$$\Gamma = \mathrm{diag}\,\left(0.033(\tfrac{m}{s}/^o), 0.033(\tfrac{m}{s}/^o), 0, 0, 0, 0.75(\tfrac{o}{s}/^o)\right)$$
$$K_{P_{egom}} = \mathrm{diag}\,(1.3789, 1.3301, 0, 0, 0, 1.0371)$$
$$K_{I_{egom}} = \mathrm{diag}\,(0.0117, 0.0117, 0, 0, 0, 0.0117)$$
$$K_{D_{egom}} = \mathrm{diag}\,(0.4023, 0.4512, 0, 0, 0, -0.1836)$$
$$K_{P_{ext\_c}} = \mathrm{diag}\,(1.3301, 1.3301, 0, 0, 0, 1.0859)$$
$$K_{I_{ext\_c}} = \mathrm{diag}\,(0.0117, 0.0117, 0, 0, 0, 0.0117)$$
$$K_{D_{ext\_c}} = \mathrm{diag}\,(0.3535, 0.4512, 0, 0, 0, -0.1836)$$
$$T_d = 0.5(s) \text{ and } T_{d_h} = 0.2(s).$$

Table 2 - Means square errors between PID control and human teleoperation

Camera position	external camera	inboard camera
x mode	$Identified$ interval: 0.1175 $non-Identified$ interval: 0.1425	$Identified$ interval: 0.1171 $non-Identified$ interval: 0.1420
y mode	$Identified$ interval: 0.1012 $non-Identified$ interval: 0.1227	$Identified$ interval: 0.0997 $non-Identified$ interval: 0.1209
ψ mode	$Identified$ interval: 0.1627 $non-Identified$ interval: 0.1973	$Identified$ interval: 0.1675 $non-Identified$ interval: 0.2031

In Fig. 10 the path following for both cases, with camera inboard and external camera was comparatively illustrated. The all-round impression is that

apparently a more tight modelling had result in the inboard-camera case. Also it could be verified by the comparative error listing in Table 3.
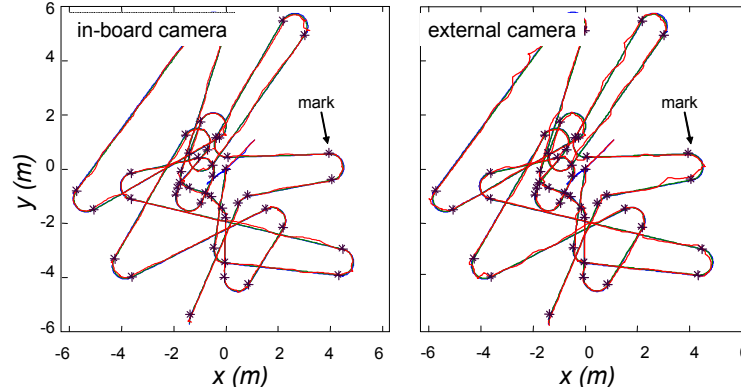

Fig. 10 Teleoperation comparison with inboard camera and external camera

Table 3 - Means-square errors in time for different motion modes

Camera position	external camera	inboard camera
x mode	0.1269	0.0876
y mode	0.1252	0.0854
ψ mode	0.1631	0.1118

4   Conclusions

In this paper an analysis of the human behavior to guide teleoperated vehicles (like ROVs) is presented and modeled in time and frequency domain. The source of information to perform teleoperation is the image motion provided independently by inboard and external cameras. Particularly, the path tracking of a sequence of marks is focused in details. The results are obtained partly by numerical simulation and partly by interaction of the teleoperator with a computer-simulated control system with a joystick and virtual video images.

We presented a nested-control-loop structure of the teleoperation composed of a high-efficient controller in the inner loop and the human control as the external loop. The main hypothesis sustained in the results is the uncoupling about the two groups. This is fulfilled if the inner control system is highly efficient in the regulation of modes and rejection of exogenous disturbances (unpredictable flows and cable tugs). One sampled-data controller algorithm with that features was presented here. The internal control system can be modeled by a linear dynamics in the whole state space (6 geometric modes and 6 rate modes).

In this way the teleoperator has to generate references for the linear system and to close the loop by means of image motion. In the paper, this human control behavior in a stationary full-learned phase has been approximated by a PID controller with estimation of the pure delays due to the image transmission and human reaction times involved. For the identification of the PID parameter there was considered to approaches: The identification in frequency and in the time domain.

A case study was worked up in order to compare properties of the human control with the simulated PID-like control, employing egomotion and external camera. In the experimentation it was obtained the online human control based on virtual image motion using a joystick to close the loop using a sampled-data model of a 6 DOF, full actuated ROV dynamics. After that, one considered a pure simulation with PID control instead of the Human teleoperation. It was shown that the PID identification is much more precise in the time domain than in the frequency domain. The obtained PID parameters were very similar between inboard and external camera. In this way the precision of the human teleoperator was analyzed in both cases of camera position.

At the present we were carrying out similar experiences in a experimental tank with a real teleoperated hybrid AUV/ROV. The results are being working up to definitive conclusions for future publication.

References

1. Jordán, M.A., Bustamante, J.L.: Adaptive Control for Guidance of Underwater Vehicles. in Underwater Vehicles, A.V. Inzartev (Editor), Chapter 14, pp. 251-278, In-Tech, Vienna, Austria (2009)
2. Kumar, R.P., Dasgupta, A., Kumar, C.S.: Robust Trajectory Control of Underwater Vehicles Using Time Delay Control Law. *Ocean Engineering,* 34 (5-6), 842-849 (2007)
3. Xiao, L., Ye, L., Yu-ru, X. , Lei, W., Zai-bai, Q.: Fuzzy neural network control of underwater vehicles based on desired state programming. *J. of Marine Science and Application,* 5 (3), 1-4 (2006)
4. Peterka, R.J.: Simplifying the Complexities of Maintaining Balance. *IEEE Engineering in Medicine and Biology Magazine*, 22 (2), 63-68 (2003)
5. Hidenori, K., Jiang, Y.: A PID model of human balance keeping. *IEEE Control Systems Magazine,* 26 (6), 18-23, (2006)
6. Ando, N., Lee, J.-H., Hashimoto, H.: A Study on Influence of Time Delay in Teleoperation. In: *Proc. of the 1999 IEEE/ASME Int. Conf. on Advanced Intelligent Mechatronics*, Atlanta, USA, Sep. 19-23, vol. 5, pp. 1111 - 1116 (1999).
7. Sheridan, T.B.: Space Teleoperation Through Time Delay: Review and Prognosis. *IEEE Transactions On Robotics And Automation*, 9 (5), 592-606 (1993)
8. Fossen, T.I.: Guidance and Control of Ocean Vehicles. John Wiley&Sons, New York (1994)
9. Jordán, M.A., Bustamante, J.L., Martinez, N., Wiener, N.: An Approach To Real-Time Animatronic Of Controlled Teleoperated Underwater Vehicles. In: 7*th Argentine Symp. on Comp. Tech. (AST 2006),* Mendoza, Argentina, Sep. 4-8, pp. 210-211 (2006)
10. Jordán, M.A., Bustamante, J.L.: Adams-Bashforth Approximations For Digital Control Of Complex Vehicle Dynamics. In: *4th Int. Scientific Conf. on Physics and Control (PHYSCON 2009)*, Catania, Italy, Sep. 1-4 (2009)
11. Jordán, M.A., Bustamante, J.L.: Guidance of Underwater Vehicles with Cable Tug Perturbations Under Fixed and Adaptive Control Modus. *IEEE J. of Oceanic Engineering*, 33(4), 579-598 (2008)
12. Jordán, M.A., Bustamante, J.L.: A Speed-Gradient Adaptive Control with State/ Disturbance Observer for Autonomous Subaquatic Vehicles. In 4*5th. IEEE Conf. on Dec. and Control*, San Diego, USA, Dec. 11-13, pp. 2008-2013, (2006)